



# Excess total organic carbon in the intermediate water of the South China Sea and its export to the North Pacific

**Minhan Dai, Feifei Meng, and Tiantian Tang**

*State Key Laboratory of Marine Environmental Science, College of Oceanography and Environmental Science, Xiamen University, Xiamen 361005, China (mdai@xmu.edu.cn)*

**Shu-Ji Kao**

*State Key Laboratory of Marine Environmental Science, College of Oceanography and Environmental Science, Xiamen University, Xiamen 361005, China*

*Also at Research Center for Environmental Changes, Academia Sinica, Taipei 11560, Taiwan*

**Jianrong Lin and Junhui Chen**

*State Key Laboratory of Marine Environmental Science, College of Oceanography and Environmental Science, Xiamen University, Xiamen 361005, China*

**Jr-Chuan Huang**

*Research Center for Environmental Changes, Academia Sinica, Taipei 11560, Taiwan*

**Jiwei Tian**

*College of Marine Environment, Ocean University of China, Qingdao 266071, China*

**Jianping Gan**

*Department of Mathematics, Atmospheric, Marine and Coastal Environment Program, School of Science, Hong Kong University of Science and Technology, Kowloon 999077, Hong Kong*

**Shuang Yang**

*State Key Laboratory of Marine Environmental Science, College of Oceanography and Environmental Science, Xiamen University, Xiamen 361005, China*

[1] Depth profiles of total organic carbon (TOC) were measured in spring (2005) and winter (2006) in the South China Sea (SCS), the largest marginal sea adjacent to the North Western Pacific (NWP). Compared to TOC profiles in the NWP, excess TOC ( $3.2 \pm 1.1 \mu\text{mol kg}^{-1}$ ) was revealed in the intermediate layer of the SCS at  $\sigma_\theta \sim 27.2\text{--}27.6$  ( $\sim 1000\text{--}1500$  m). Below the depth of 2000 m, TOC concentrations were identical between the SCS and the NWP. Based on a one-dimensional steady state diffusion advection model constrained by potential temperature, we estimated a net TOC production rate of  $0.12 \pm 0.04 \mu\text{mol kg}^{-1} \text{yr}^{-1}$  to maintain this excess. A positive relationship between TOC and apparent oxygen utilization in the SCS deep water lent support to such a model-derived TOC production. This excess TOC in the out-flowing intermediate water may carry  $3.1 \pm 2.1 \text{Tg C yr}^{-1}$  of organic carbon out from the SCS and potentially into the deep open ocean. In light of the short residence time of the SCS deep water, the exported TOC was likely from the recently fixed organic carbon within the SCS. The export of such organic carbon, thereby less likely to return to the atmosphere may therefore contribute significantly to the carbon sequestration in the SCS.

**Components:** 4645 words, 4 figures.

**Keywords:** TOC; marginal seas; intermediate water.

**Index Terms:** 4806 Oceanography: Biological and Chemical: Carbon cycling (0428); 4243 Oceanography: General: Marginal and semi-enclosed seas; 4219 Oceanography: General: Continental shelf and slope processes (3002).

**Received** 27 July 2009; **Revised** 18 September 2009; **Accepted** 6 October 2009; **Published** 2 December 2009.

Dai, M., F. Meng, T. Tang, S.-J. Kao, J. Lin, J. Chen, J.-C. Huang, J. Tian, J. Gan, and S. Yang (2009), Excess total organic carbon in the intermediate water of the South China Sea and its export to the North Pacific, *Geochem. Geophys. Geosyst.*, 10, Q12002, doi:10.1029/2009GC002752.

## 1. Introduction

[2] Dissolved organic carbon (DOC) is a critically important component in oceanic carbon cycling, representing one of the largest pools of organic carbon in the biosphere, the stock of which ( $\sim 700 \times 10^{15}$  g C) is close to that of atmospheric CO<sub>2</sub> ( $\sim 750 \times 10^{15}$  g C) [Siegenthaler and Sarmiento, 1993]. However, our understanding of the source and the fate of marine DOC as well as its bioavailability, remains very limited. Net DOC production that escapes rapid microbial utilization and accumulates in the surface water is available for export to the ocean interior, and this part of the DOC is estimated to be 1.2 Gt C year<sup>-1</sup> or 17% of global new production each year [Hansell and Carlson, 1998a].

[3] While a large fraction of DOC in the deep ocean may originate from the surface ocean at the sites of deep water formation [Hansell and Carlson, 1998b], there is evidence that deep ocean DOC may also come from marginal seas, which generally produce more organic carbon than they can respire [Smith and Hollibaugh, 1993], implying that a fraction of this organic carbon may be transported vertically to the deep and/or horizontally with the outflow of subsurface water [Deng et al., 2006; Tsunogai et al., 1999], or sediment gravity flows [Canals et al., 2006] from the sites of formation. Hansell and Carlson [1998b] suggest that along the deep path of the global “conveyor belt,” additional DOC is loaded by isopycnal and diapycnal eddy diffusion either from the marginal sea or the surface ocean. Note that compared to carbon in the particulate form, the enrichment of carbon relative to the Redfield ratio in the DOC pool makes its export to the open ocean interior to sequester carbon more efficient [Hopkinson and Vallino, 2005], particularly when the export is along the isopycnal layer.

[4] The South China Sea (SCS) is the largest subtropical-tropic marginal sea in the world, with an area of about  $3.5 \times 10^6$  km<sup>2</sup> [Hu et al., 2000]. The Luzon Strait (the deepest sill at  $\sim 2400$  m) is the only opening for deepwater exchange between the SCS and the adjacent North Western Pacific (NWP) [Qu et al., 2006]. It has been well documented that water exchange across the Luzon Strait exhibits a “sandwich-like” flow pattern, with an inflow from the NWP in the upper and deeper layers but an outflow to the NWP in the intermediate layer [Chao et al., 1996; Li and Qu, 2006; Qu et al., 2006; Tian et al., 2006; Gan et al., 2006]. In terms of mass balance, the rapid replenishment of the SCS deep water from the NWP is maintained by fast ventilation with the shallower intermediate water, as well as a persistent net outflow at an intermediate depth [Chao et al., 1996; Chen et al., 2006; Li and Qu, 2006]. According to Chou et al. [2007], this intermediate outflow exports  $17.6 \pm 9$  Tg C yr<sup>-1</sup> from the SCS in the dissolved inorganic carbon form, accounting for  $35 \pm 18\%$  of the annual export production in the SCS.

[5] This is the first study to present depth profiles of DOC covering a large spatial area in the SCS. A basin-wide enrichment of DOC was observed in the intermediate layer and simulated using a one-dimensional steady state diffusion advection model. Such excess DOC may readily be exported from the marginal sea to the adjacent open ocean, which may represent an important pathway to sequester carbon within the SCS and a critically important carbon source of the interior Pacific Ocean.

## 2. Material and Methods

### 2.1. Sampling and Analysis

[6] Data were collected during April–May 2005 and November–December 2006, covering the

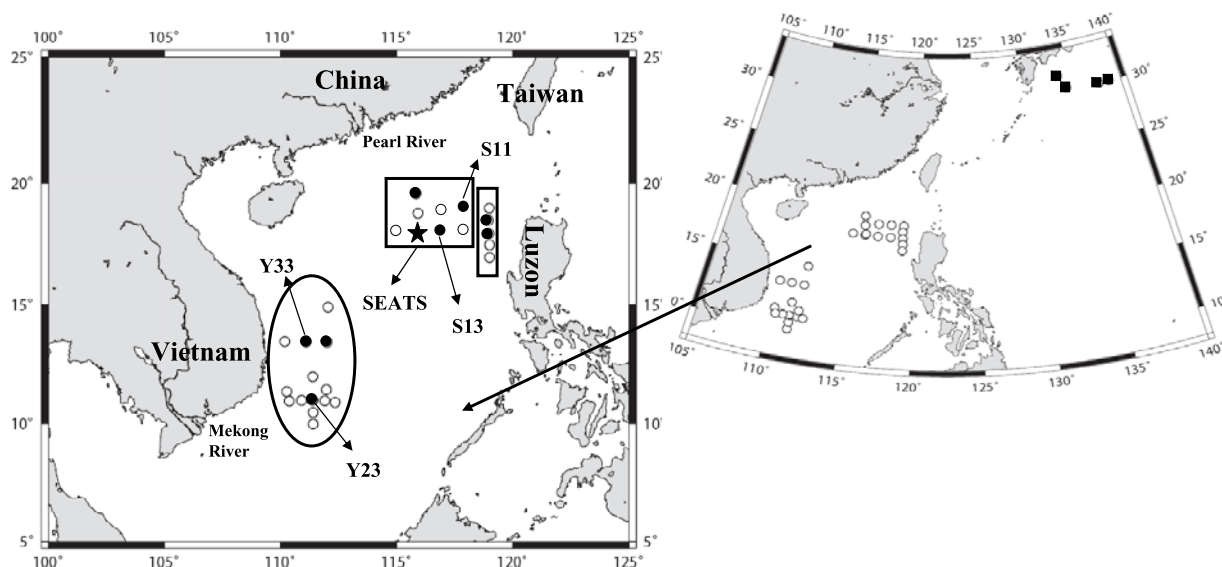


**Figure 1.** Map of the South China Sea (SCS) and sampling sites in the western SCS off Vietnam (elliptic zone), northeastern SCS off Luzon (vertical quadrante zone), and in the northern SCS basin (horizontal quadrante zone). The closed symbols are the locations of the vertical profiles discussed. The reference stations (see section 2.2.1) in the northwestern Pacific (NWP) are shown in solid squares.

northern, western (off Vietnam) and eastern (off Luzon) SCS basin (Figure 1). The water depth of the stations considered in this study all exceeded 2000 m. Depth profiles of temperature and salinity were recorded with a calibrated SeaBird conductivity-temperature-depth (CTD) recorder (model SBE9/11).

[7] Samples were collected in triplicate using 12 L GoFlo bottles attached to the CTD rosette following the JGOFS protocol [Sharp *et al.*, 1995]. Nonfiltered water samples were stored in precombusted EPA vials at  $-20^{\circ}\text{C}$  until TOC (total organic carbon) was measured (DOC may represent  $> 97\%$  of TOC in our study area) using a Shimadzu TOC-V Analyzer. Before measuring samples, a four-point standard curve was performed on a daily basis by injection of standard solutions of potassium hydrogen phthalate. Quality assessment was done using consensus reference waters, consisting of a low-carbon water ( $1\text{--}2\ \mu\text{mol C L}^{-1}$ ) and a deep Sargasso Seawater ( $44\text{--}46\ \mu\text{mol C L}^{-1}$ ), provided by Dennis Hansell's laboratory at the University of Miami (<http://www.rsmas.miami.edu/groups/biogeochem/CRM.html>). The coefficient of variation on the analysis of our replicate measurements was approximately 2%. Deep Sargasso Seawater variability (standard deviation) throughout our measuring time series record was  $\pm 0.8\ \mu\text{mol C L}^{-1}$  ( $n = 114$ ), useful as an index of our analytical precision.

## 2.2. Literature Data Source

### 2.2.1. Reference Stations in the NWP

[8] Hydrological and TOC data for the reference stations in the NWP ( $133^{\circ}49'\text{E}$ ,  $31^{\circ}28'\text{N}$ ;  $138^{\circ}47'\text{E}$ ,  $30^{\circ}\text{N}$ ;  $137^{\circ}45'\text{E}$ ,  $30^{\circ}\text{N}$ ;  $134^{\circ}29'\text{E}$ ,  $30^{\circ}\text{N}$ ) (Figure 1) are from [http://cdiac.esd.ornl.gov/oceans/RepeatSections/clivar\\_p02.html](http://cdiac.esd.ornl.gov/oceans/RepeatSections/clivar_p02.html). These data were collected in June 2004.

### 2.2.2. Volume Transport

[9] The net volume transport through the Luzon Strait was reestimated based on Tian *et al.* [2006] by integrating the subinertial velocity along the column depth and the strait width. In practice, the strait width varied much at different depths, and were derived from the ETOP2 bathymetry data. The velocity profiles for zonal flow were fit to the subinertial flow, semidiurnal tide, and diurnal tide using the least square method.

## 2.3. One-Dimensional Diffusion Advection Model

[10] In order to examine the potential source of the excess TOC, a one-dimensional steady state diffusion advection model proposed by Craig [1969] was adapted for the depth of 500–2500 m in deep SCS water. The model assumed that the vertical profile of the dissolved component was a two-point

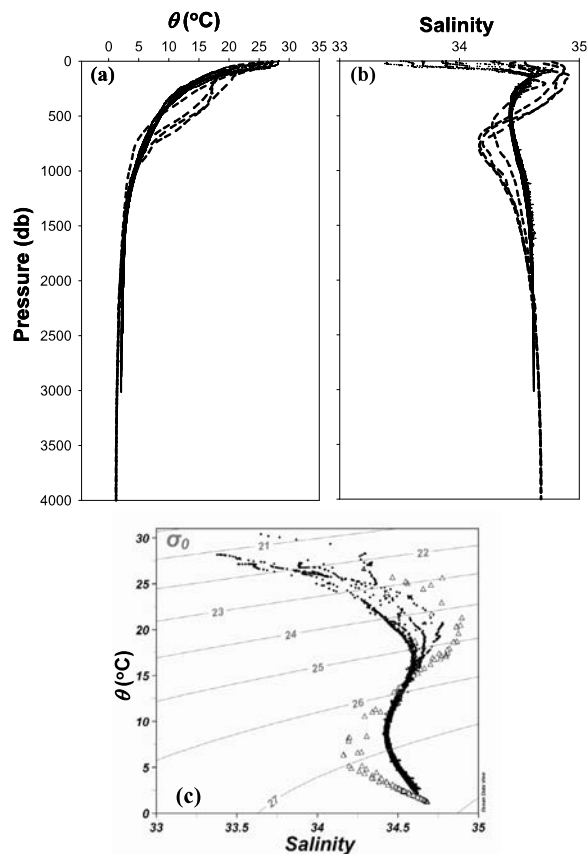


**Figure 2.** Vertical profiles of (a) potential temperature ( $\theta$ ) and (b) salinity. Solid dots and black dashed curves in Figures 2a and 2b represent the data from the SCS and profiles from the NWP, respectively. (c) The relationships of  $\theta$ -S for the stations located in the SCS (black dots) and the NWP (open triangles). The Pacific data are from [http://cdiac.esd.ornl.gov/oceans/RepeatSections/clivar\\_p02.html](http://cdiac.esd.ornl.gov/oceans/RepeatSections/clivar_p02.html).

boundary value, without any consideration of interior horizontal processes. The model was thus applicable where the potential temperature-salinity ( $\theta$ -S) relationship was linear.

[11] For a conservative tracer, the vertical profile can be expressed by

$$\theta = \theta_0 + (\theta_m - \theta_0)f(z) \quad (1)$$

where  $f(z) = (\exp(z/z^*) - 1)/(\exp(z_m/z^*) - 1)$ ;  $z$  is the vertical coordinate (positive upward), and  $z^*$  is the mixing parameter defined by  $z^* = K/w$ ;  $K$  is the vertical eddy diffusion coefficient in  $\text{m}^2 \text{s}^{-1}$ ; and  $w$  is the upward advection velocity in  $\text{m s}^{-1}$ .  $K$  and  $w$  values were assumed to be independent of depth. When  $\theta = \theta_0$  at  $z = 0$  (at the bottom), we have  $\theta = \theta_m$  at  $z = z_m$  (at the top).

[12] Other than vertical mixing, profiles of non-conservative tracers, such as TOC, can be modified by on site production and consumption processes in water columns. Following *Craig* [1969], we added a  $J$  term into the equation for a stable, nonconservative tracer:

$$C = C_0 + (C_m - C_0)f(z) - J/w[z - z_m f(z)]. \quad (2)$$

where  $C(0) = C_0$ ;  $C(z_m) = C_m$ ; and  $J$  is in  $\mu\text{mol kg}^{-1} \text{yr}^{-1}$ . Negative and positive values in the  $J$  term indicate the net consumption and production rate, respectively.

### 3. Results and Discussion

#### 3.1. Hydrography

[13] The vertical profiles of  $\theta$  and  $S$  are shown in Figures 2a and 2b, respectively for both the SCS and the NWP, and the water properties in the upper 2000 m are distinctively different between the two basins. The lower surface  $S$  in the SCS is attributable to the basin-wide precipitation and the input from large rivers (i.e., the Pearl River and Mekong River) [*Wyrski*, 1961]. In the subsurface layer (from 100 to 700 m), the  $\theta$  in the SCS was considerably lower than that in the NWP. The  $S$  maximum in the SCS occurred at 150 m, the same depth as that in the NWP (though less intensive). However, the  $S$  minimum in the SCS was located at a depth of 500 m, which is shallower than that in the NWP ( $\sim 750$  m), but the value was higher. It is believed that the  $S$  maximum and minimum in the SCS are influenced, respectively, by North Pacific tropical water and the intermediate water sourced from the subpolar region [*You*, 2003]. The hydrography of the SCS was homogeneous below 2000 m and identical to that at  $\sim 2000$  m in the NWP (Figures 2a and 2b). The characteristics of the SCS deep water are also shown in the  $\theta$ -S diagram (Figure 2c), which suggests that the deep SCS water was indeed of North Pacific (NP) origin as reported previously [*Chen et al.*, 2006; *Gong et al.*, 1992; *Wang*, 1986]. Due to the enhanced vertical mixing, the overall SCS water  $\theta$ -S property showed a less curved inverse “S” shape as compared to the  $\theta$ -S relationship in the NWP (Figure 2c).

#### 3.2. Comparison of TOC Distributions Between the SCS and the NWP

[14] Vertical profiles of TOC generally showed a pattern of high concentrations in the mixed

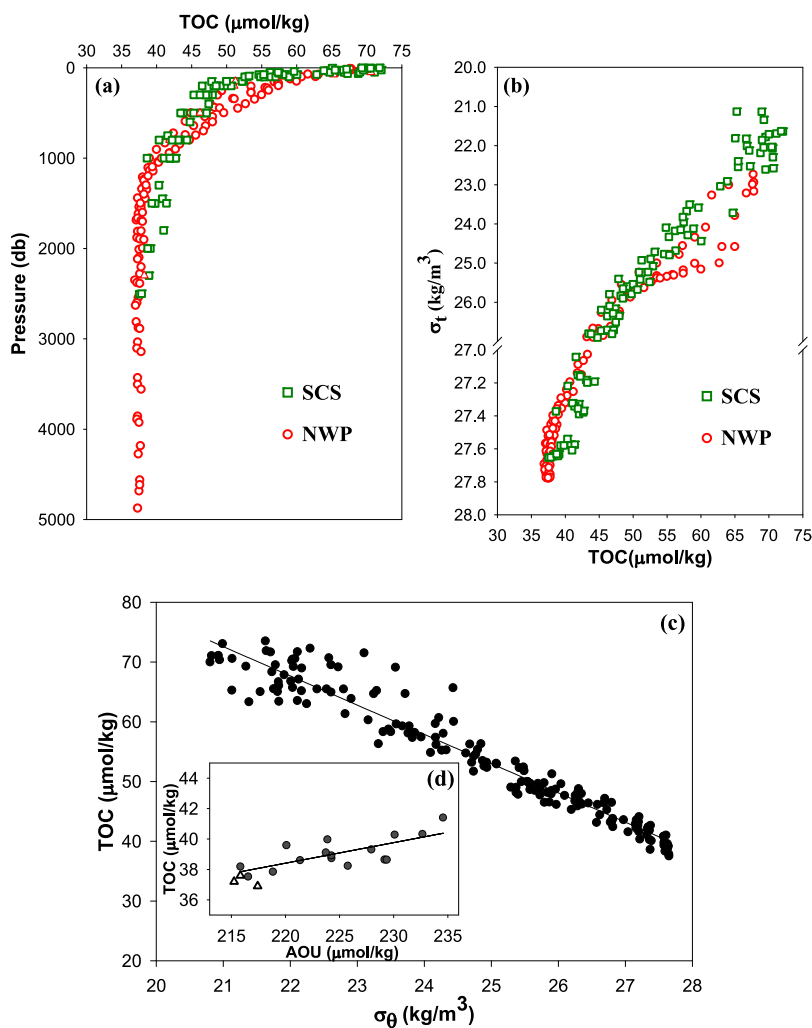


**Figure 3.** (a) Depth profiles of TOC for stations in the NWP and in the SCS. (b) Potential density ( $\sigma_{\theta}$ ) versus TOC for all corresponding samples in Figure 3a. (c) Scatterplots of TOC versus  $\sigma_{\theta}$  in the SCS. (d) TOC versus AOU in the deep SCS water, where samples below 1000 m (dark gray dots) were selected and samples below 2200 m of the NWP (open triangles) are shown for reference. The Pacific data are from [http://cdiac.esd.ornl.gov/oceans/RepeatSections/clivar\\_p02.html](http://cdiac.esd.ornl.gov/oceans/RepeatSections/clivar_p02.html).

layer ( $65\text{--}72 \mu\text{mol kg}^{-1}$ ) with a sharp decline to  $\sim 50 \mu\text{mol kg}^{-1}$  in the upper 100 m. At 1000–2000 m, a small but consistent vertical TOC gradient existed from  $41.6 \pm 0.9$  to  $38.4 \pm 0.5 \mu\text{mol kg}^{-1}$ . No clear seasonal trends and/or spatial differences in TOC concentrations were observed among stations at the same depth interval. The distribution of TOC in the SCS appears to be primarily controlled by physical processes as manifested by a statistically significant negative correlation between TOC and density ( $\sigma_{\theta}$ ) [TOC =  $(-4.9 \pm 0.093) \sigma_{\theta} + (175.4 \pm 2.3)$ ,  $r = 0.97$ ,  $p < 0.0001$ ,  $n = 172$ ] (Figure 3c).

[15] As compared to the NWP, TOC in the upper 1000 m of the SCS was generally lower (Figure 3a).

Such a deficit in TOC might be caused by rapid ventilation with the TOC-depleted deep water [Qu *et al.*, 2006]. The TOC concentration below 2000 m showed a very narrow range of  $38.4 \pm 0.5 \mu\text{mol kg}^{-1}$  in the SCS without significant spatial and temporal differences, comparable with that in the intermediate water of the subtropical Pacific (TOC =  $38.7 \pm 0.7 \mu\text{mol kg}^{-1}$  [Hansell *et al.*, 2002]). Such an identical TOC concentration confirmed a rapid deepwater exchange between the two basins, which is also indicated based on the insignificant difference between the SCS and the NWP in  $\Delta^{14}\text{C}$  below 1500 m [Broecker *et al.*, 1986]. The most important feature of the TOC profiles between the SCS and the NWP was that there was a TOC “bump” in the intermediate SCS water ( $\sim 1000\text{--}$

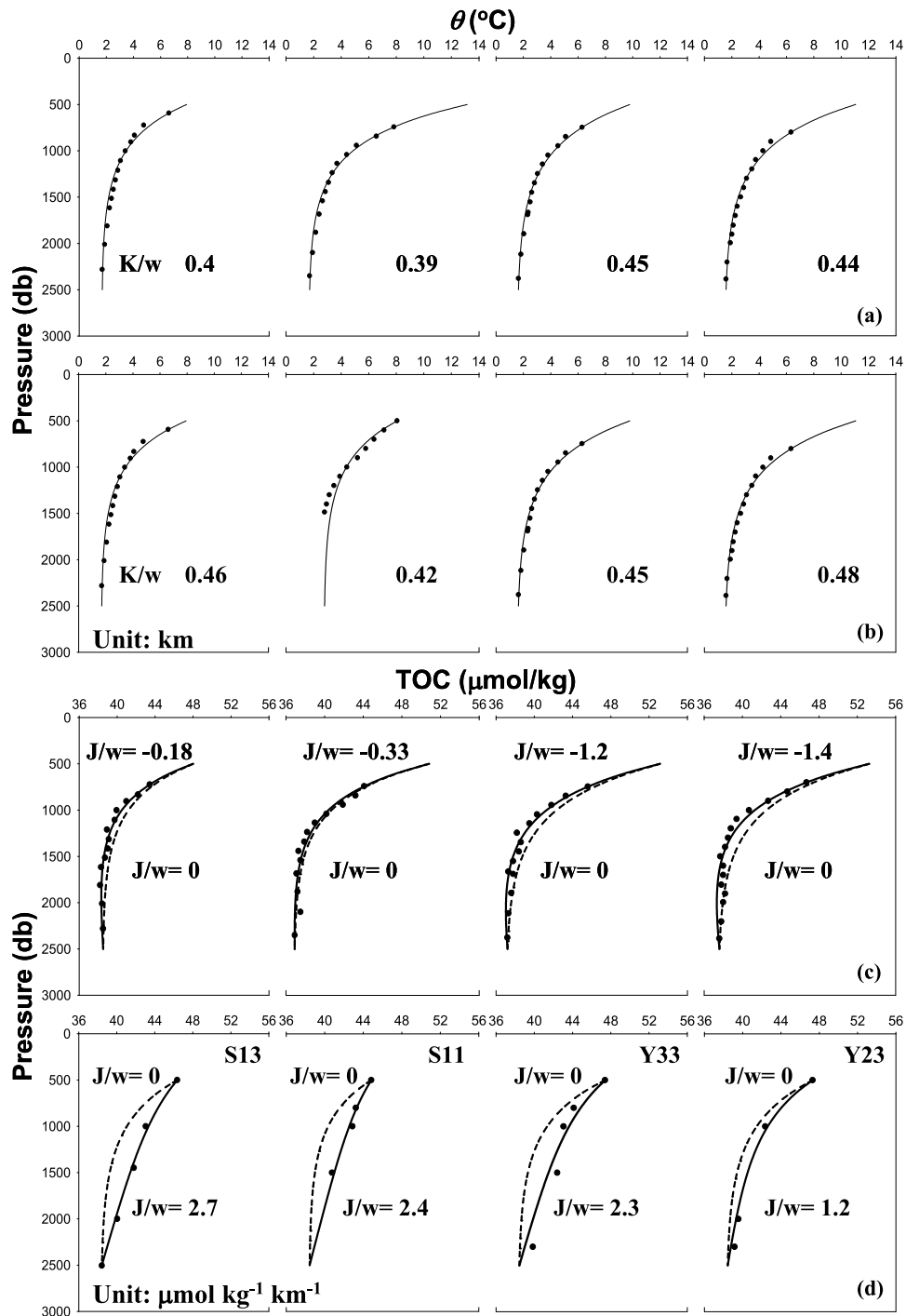


**Figure 4.** Profiles of  $\theta$  (dots) for (a) the NWP and (b) the SCS. Note that S13 and S11 are in the northern SCS basin, and Y33 and Y23 are the stations off Vietnam. See Figure 1 for station locations. Model derived  $K/w$  values were obtained through fitting the  $\theta$  curves. (c and d) The observed TOC (dots) and modeled profiles under different  $J/w$  values (see section 3.3 for details). The Pacific data are from [http://cdiac.esd.ornl.gov/oceans/RepeatSections/clivar\\_p02.html](http://cdiac.esd.ornl.gov/oceans/RepeatSections/clivar_p02.html).

1500 m,  $\sigma_{\theta} = 27.2\text{--}27.6$  (Figures 3a and 3b)). Note that in the North Pacific, the TOC below 1000 m was typically uniform. For example, along  $152^{\circ}\text{W}$  from  $30^{\circ}\text{N}$  to  $10^{\circ}\text{N}$ , a TOC average of  $37.4 \pm$

$0.8 \mu\text{mol kg}^{-1}$  ( $n = 255$ , [http://cdiac.esd.ornl.gov/oceans/RepeatSections/clivar\\_p16n.html](http://cdiac.esd.ornl.gov/oceans/RepeatSections/clivar_p16n.html)) can be obtained, which agreed well with that of the reference stations in the NWP ( $38.0 \pm 0.8 \mu\text{mol}$

kg<sup>-1</sup>). The enrichment of TOC in the SCS was therefore statistically valid with an increment of  $3.2 \pm 1.1 \mu\text{mol kg}^{-1}$  ( $t$  test,  $\alpha = 0.000$ ) (Figures 3a and 3b).

### 3.3. Model Results

[16] At a water depth between  $\sim 500$  and 2500 m in the SCS, the  $\theta$ -S diagram showed a relatively linear correlation (Figure 2c), suggesting that our vertical diffusion model had applicability at this depth horizon. We then obtained the ratio,  $z^* = K/w$  (units in km (see Figures 4a and 4b)) from the integration of equation (1), and the observed  $\theta$  curve using least squares fitting. The range of  $z^*$  in the NWP was 0.39–0.45 km (Figure 4a) and in the SCS was 0.42–0.48 km (Figure 4b). Though the  $z^*$  values were similar in the two basins, the abyssal water upwelling rate (i.e.,  $w$ ) in the SCS was much higher ( $55 \text{ m yr}^{-1}$  [Chen *et al.*, 2001]) as compared to that reported in the NP ( $4.5 \text{ m yr}^{-1}$  [Craig, 1969]). This basin-wide high upwelling rate in the SCS is attributed to a persistent counterclockwise circulation around the depth interval of 1000–2000 m with respect to 2500 m [Wang, 1986].

[17] Figures 4c and 4d compared the vertical TOC profiles of the SCS with those of the NWP. Using the parameters shown by earlier simulation, we obtained the best fit  $J/w$  values (black curves) for the observed TOC profiles. Theoretical curves (dashed curves) calculated from equation (2) of  $J = 0$  (pure mixing) are shown for comparison (Figures 4c and 4d). We utilized  $55 \text{ m yr}^{-1}$  [Chen *et al.*, 2001] and  $4.5 \text{ m yr}^{-1}$  [Craig, 1969], respectively, for  $w$  values in the SCS and the NWP to calculate  $J_{\text{TOC}}$ . The average  $J_{\text{TOC}}$  of the NWP was estimated to be  $-0.0042 \pm 0.0021 \mu\text{mol kg}^{-1} \text{ yr}^{-1}$ . By contrast, the mean  $J_{\text{TOC}}$  in the SCS was  $0.12 \pm 0.04 \mu\text{mol kg}^{-1} \text{ yr}^{-1}$  indicating production. The water in the SCS proper, say at 2000 m, was between 40 and 52 years older than the source water [Chen *et al.*, 2001]. Using this residence time and the model-derived TOC production rate, we obtained a concentration of  $5.5 \pm 2.0 \mu\text{mol kg}^{-1}$ . This value represented the total TOC accumulated in the intermediate layer over 40–52 years and agreed well with the observed excess TOC ( $3.2 \pm 1.1 \mu\text{mol kg}^{-1}$ ) around the same depth.

[18] The consistency between model results and field observations indicated that an additional source of TOC had been introduced into the intermediate layer of the SCS. This was probably a consequence of the breakdown/consumption of sinking particles. The small but consistent vertical

TOC gradient of  $\sim 3 \mu\text{mol kg}^{-1}$  at 1000–2000 m (Figure 3a) may provide evidence that continual sinking and degradation of organic carbon occurred below 1000 m. Moreover, we found a generally significant positive linear correlation (Figure 3d) between TOC and apparent oxygen utilization (AOU) ( $r = 0.73$ ,  $p = 0.0014$ ,  $n = 14$ ) in the deep SCS water below 1000 m. Kumar [1990] suggests that the correlation between TOC and AOU can be negative or positive depending upon which process is relatively more important, the breakdown of sinking particle to TOC, or oxidation of TOC to  $\text{CO}_2$ . Another possibility may be diapycnal mixing between the intermediate water with high TOC and low oxygen, and the deep water along with relatively lower TOC and higher oxygen, which was comparable to the water below 2200 m in the NWP (see open triangles in Figure 3d). Recently, Yamashita and Tanoue [2008] observe that fluorescence intensity and AOU are linearly correlated in the mesopelagic and abyssal layers of the interior of the Pacific Ocean. They conclude that fluorescent dissolved organic matter is produced in situ in the ocean interior as organic matter is oxidized biologically. Our results gave a similar positive correlation for TOC against AOU, which might suggest that a similar process had occurred in the SCS (preliminary study showed that fluorescence intensity also correlates positively with AOU in our study area). Compared with the Pacific and the Atlantic Ocean [Broecker *et al.*, 1991; Sarmiento and Gruber, 2006], a three times higher deep ocean oxygen utilization rate (below 2000 m) is observed in the SCS [Lin *et al.*, 1996], which is ascribed to higher export of organic matter from the surface [Sarmiento and Gruber, 2006].

[19] The excess TOC ( $3.2 \pm 1.1 \mu\text{mol kg}^{-1}$ ) observed in this study, together with the net water flux between 1000 m to 1500 m of  $2.5 \pm 1.5 \text{ Sv}$  (reestimated based on Tian *et al.* [2006]), supported that the intermediate outflow could export  $3.1 \pm 2.1 \text{ Tg C yr}^{-1}$  ( $1 \text{ Tg} = 10^{12} \text{ g}$ ) in TOC form from the SCS. Although the above estimate may be subject to considerable uncertainties, due primarily to the error in the estimate of the water flux, our result demonstrated that water exchanges through the Luzon Strait may represent an alternative pathway in exporting organic carbon from the deep SCS.

## 4. Summary

[20] Physical mixing dominates TOC distribution in the SCS. A one-dimensional steady state diffusion advection model revealed that a net TOC

production rate of  $\sim 0.12 \pm 0.04 \mu\text{mol kg}^{-1} \text{yr}^{-1}$  was required to maintain the excess TOC ( $3.2 \pm 1.1 \mu\text{mol kg}^{-1}$ ) in the intermediate layer ( $\sigma_\theta = 27.2\text{--}27.6$ ,  $\sim 1000\text{--}1500$  m). The origin of this TOC was unclear, but, when compared with the ambient water in the NWP, SCS intermediate water outflow ( $2.5 \pm 1.5$  Sv) acted as a source of TOC, transporting  $3.1 \pm 2.1$  Tg organic carbon to the North Pacific interior annually.

[21] There may be two implications with respect to this export of organic carbon from a marginal sea system. Given the fact that the residence time of the SCS deep water is short (less than 30 years [Qu *et al.*, 2006]), the exported TOC was likely from the recently fixed organic carbon within the SCS. The export of such organic carbon, thereby less likely to return to the atmosphere may therefore contribute significantly to the carbon sequestration in the South China Sea. At the same time, this relatively freshly produced organic carbon, when exported into the adjacent open ocean interior might also contribute to a deep ocean organic carbon pool. It must be pointed out that more studies are mandatory in order to fully understand the fate of this newly found excess TOC and to explore its transformation processes during transportation. Also needed is to evaluate the significance of TOC exported from marginal seas and its contribution to the deep organic carbon reservoir at a global scale.

## Acknowledgments

[22] We would like to thank X. Guo, W. Zhai and J. Hu for help with the ancillary data collection. This work was supported by the National Basic Research Program of China (973 Program), Ministry of Science and Technology, through grant 2009CB421200 and by the National Science Foundation of China (NSFC) through grants 40821063, 90711005, and 40490264. Thanks are also extended to K. K. Liu and C. Lee for their inspiring comments during the preparation of the manuscript. John Hodgkiss is thanked for his assistance with English. D. A. Hansell and an anonymous reviewer provided valuable comments that improved the manuscript.

## References

- Broecker, W. S., W. C. Patzert, J. R. Toggweiler, and M. Stuiver (1986), Hydrography, chemistry, and radioisotopes in the Southeast Asian basins, *J. Geophys. Res.*, *91*, 14,345–14,354, doi:10.1029/JC091iC12p14345.
- Broecker, W. S., W. C. Patzert, J. R. Toggweiler, and M. Stuiver (1991), Radiocarbon decay and oxygen utilization in the deep Atlantic Ocean, *Global Biogeochem. Cycles*, *5*, 87–117, doi:10.1029/90GB02279.
- Canals, M., P. Puig, X. D. de Madron, S. Heussner, A. Palanquer, and J. Fabres (2006), Flushing submarine canyons, *Nature*, *444*, 354–357, doi:10.1038/nature05271.
- Chao, S. Y., P. T. Shaw, and S. Y. Wu (1996), Deep water ventilation in the South China Sea, *Deep Sea Res., Part I*, *43*, 445–466, doi:10.1016/0967-0637(96)00025-8.
- Chen, C. T. A., S. L. Wang, B. J. Wang, and S. C. Pai (2001), Nutrient budgets for the South China Sea basin, *Mar. Chem.*, *75*, 281–300, doi:10.1016/S0304-4203(01)00041-X.
- Chen, C. T. A., W. P. Hou, T. Gamo, and S. L. Wang (2006), Carbon-related parameters of subsurface waters in the West Philippine, South China Sea and Sulu seas, *Mar. Chem.*, *99*, 151–161, doi:10.1016/j.marchem.2005.05.008.
- Chou, W. C., D. D. Sheu, C. T. A. Chen, L. S. Wen, Y. Yang, and C. L. Wei (2007), Transport of the South China Sea subsurface water outflow and its influence on carbon chemistry of Kuroshio waters off southeastern Taiwan, *J. Geophys. Res.*, *112*, C12008, doi:10.1029/2007JC004087.
- Craig, H. (1969), Abyssal carbon and radiocarbon in the Pacific, *J. Geophys. Res.*, *74*, 5491–5506, doi:10.1029/JC074i023p05491.
- Deng, B., J. Zhang, and Y. Wu (2006), Recent sediment accumulation and carbon burial in the East China Sea, *Global Biogeochem. Cycles*, *20*, GB3014, doi:10.1029/2005GB002559.
- Gan, J., H. Li, E. N. Curchitser, and D. B. Haidvogel (2006), Modeling South China Sea circulation: Response to seasonal forcing regimes, *J. Geophys. Res.*, *111*, C06034, doi:10.1029/2005JC003298.
- Gong, G. C., K. K. Liu, C. T. Liu, and S. C. Pai (1992), The chemical hydrography of the South China Sea west of Luzon and a comparison with the West Philippine Sea, *Terr. Atmos. Oceanic Sci.*, *3*, 587–602.
- Hansell, D. A., and C. A. Carlson (1998a), Net community production of dissolved organic carbon, *Global Biogeochem. Cycles*, *12*, 443–453, doi:10.1029/98GB01928.
- Hansell, D. A., and C. A. Carlson (1998b), Deep ocean gradients in the concentration of dissolved organic carbon, *Nature*, *395*, 263–266, doi:10.1038/26200.
- Hansell, D. A., C. A. Carlson, and Y. Suzuki (2002), Dissolved organic carbon export with North Pacific Intermediate Water formation, *Global Biogeochem. Cycles*, *16*(1), 1007, doi:10.1029/2000GB001361.
- Hopkinson, C. S., and J. J. Vallino (2005), Efficient export of carbon to the deep ocean through dissolved organic matter, *Nature*, *433*, 142–145, doi:10.1038/nature03191.
- Hu, J., H. Kawamura, H. Hong, and Y. Qi (2000), A review on the currents in the South China Sea: Seasonal circulation, South China Sea Warm Current and Kuroshio Intrusion, *J. Oceanogr.*, *56*, 607–624, doi:10.1023/A:1011117531252.
- Kumar, D. (1990), Dynamics of dissolved organic carbon in the northwestern Indian Ocean, *Mar. Chem.*, *30*, 299–316, doi:10.1016/0304-4203(90)90044-D.
- Li, L., and T. Qu (2006), Thermohaline circulation in the deep South China Sea basin inferred from oxygen distributions, *J. Geophys. Res.*, *111*, C05017, doi:10.1029/2005JC003164.
- Lin, H., W. Han, and Y. Cai (1996), The consumption rate of dissolved oxygen in abyssal basin water of the northeastern South China Sea (in Chinese), *Oceanogr. China*, *6*, 103–108.
- Qu, T. D., J. B. Girton, and J. A. Whitehead (2006), Deepwater overflow through Luzon Strait, *J. Geophys. Res.*, *111*, C01002, doi:10.1029/2005JC003139.
- Sarmiento, J. L., and N. Gruber (2006), *Ocean Biogeochemical Dynamics*, 562 pp., Princeton Univ. Press, Princeton, N. J.
- Sharp, J. H., R. Benner, L. Bennett, C. A. Carlson, S. E. Fitzwater, E. T. Peltzer, and L. M. Tupas (1995), Analyses of dissolved organic carbon in seawater: The JGOFS EqPac





- methods comparison, *Mar. Chem.*, *48*, 91–108, doi:10.1016/0304-4203(94)00040-K.
- Siegenthaler, U., and J. L. Sarmiento (1993), Atmospheric carbon dioxide and the ocean, *Nature*, *365*, 119–125, doi:10.1038/365119a0.
- Smith, S. V., and J. T. Hollibaugh (1993), Coastal metabolism and the oceanic organic carbon balance, *Rev. Geophys.*, *31*, 75–89, doi:10.1029/92RG02584.
- Tian, J. W., Q. X. Yang, X. F. Liang, L. L. Xie, D. X. Hu, F. Wang, and T. D. Qu (2006), Observation of Luzon Strait transport, *Geophys. Res. Lett.*, *33*, L19607, doi:10.1029/2006GL026272.
- Tsunogai, S., S. Watanabe, and T. Sato (1999), Is there a “continental shelf pump” for the absorption of atmospheric CO<sub>2</sub>?, *Tellus, Ser. B*, *51*, 701–712, doi:10.1034/j.1600-0889.1999.t01-2-00010.x.
- Wang, J. (1986), Observation of abyssal flows in the northern South China Sea, *Acta Oceanogr. Taiwanica*, *16*, 36–45.
- Wyrki, K. (1961), Physical oceanography of the southeast Asian waters, *Naga Rep.*, *2*, 195 pp., Scripps Inst. of Oceanogr., La Jolla, Calif.
- Yamashita, Y., and E. Tanoue (2008), Production of bio-refractory fluorescent dissolved organic matter in the ocean interior, *Nat. Geosci.*, *1*, 579–582, doi:10.1038/ngeo279.
- You, Y. (2003), The pathway and circulation of North Pacific Intermediate Water, *Geophys. Res. Lett.*, *30*(24), 2291, doi:10.1029/2003GL018561.